JACS
JOURNAL OF THE AMERICAN CHEMICAL SOCIETY

COMMUNICATION

pubs.acs.org/JACS

Hierarchically Porous Silver Monoliths from Colloidal Bicontinuous Interfacially Jammed Emulsion Gels

Matthew N. Lee and Ali Mohraz*

Department of Chemical Engineering & Materials Science, 916 Engineering Tower, University of California, Irvine, California 92697, United States

Supporting Information

ABSTRACT: Silver monoliths with interconnected hierarchical pore networks and three-dimensional (3D) bicontinuous morphology are synthesized from a colloidal bicontinuous interfacially jammed emulsion gel (bijel) via reduction of silver ions within a nanoporous cross-linked polymer template. The pore sizes may be tuned independently and range from tens of nanometers to over a hundred micrometers. The method is straightforward as well as flexible and can pave the way to a host of hierarchical materials for current technologies.

Porous metallic frameworks, particularly those made of silver and gold, have widespread utility in catalysis,[1] electrochemical systems,[2] and environmental engineering,[3] and several routes to their production have been reported in the past decade. Mann et al. were first to produce macroporous silver sponges from ionic liquids using polysaccharide templates,[4] and similar approaches using chemical surfactants and hydrogels were later developed.[5−7] Erlebacher et al. established dealloying of gold/silver mixtures as a useful route to nanoporous gold with bicontinuous morphology and performed multiple dealloying steps to produce a hierarchical structure with a bimodal pore size distribution.[8−10] Such metallic structures with hierarchical pore morphology are of great interest for a number of technological applications. For example, combining interconnected pores at the nanometer and micrometer scales offers the potential to optimize both the electrochemically active surface area and the rate of fluid (or macromolecular solution) throughput to engineer the next generation of high performance batteries, microfluidic sensors, desalination membranes, catalyst supports, fuel cells, or any other process that involves simultaneous mass transport and electrochemical/electrokinetic phenomena in porous media.[11−14] To fully realize the potential of hierarchically porous materials in these applications, robust and inexpensive methods for their synthesis with controlled pore size distribution are needed. However, current methods to synthesize such materials each face important limitations. For example, the largest attainable pore size separation through the dealloying route is, to our knowledge, 2 orders of magnitude, and this method is only applicable to thin ($\leq 1\,\mu$m) sheets of material. On the other hand, recent methods based on colloidal crystal templating or controlled drying of particulate suspensions can provide access to a wider range of length scales and macroscopic 3D specimens, but the nonuniform pore geometry (spherical pockets interconnected by interstitial windows) puts stringent limits on mass transport through the structure.[15,16] Here we report a means to synthesize a novel class of hierarchically porous metallic monoliths with bicontinuous architecture on two distinct, independently tunable length scales, extending the library of such materials to those with macroscopic thickness and uniform pore channels of adjustable size ratio over a broad range suitable for the above-mentioned applications. The use of spinodal-like morphologies in these systems may allow the unique characteristics of minimal surface structures, *e.g.* enhanced transport properties, to be exploited in a hierarchical manner.[17] We tune the pore channel diameters independently while preserving the 3D spinodal morphology. Here, the sample thickness is not limited to thin films and can be several millimeters (shown here), or possibly larger. Additionally, the available pore sizes span nearly 4 orders of magnitude, from tens of nanometers to over a hundred micrometers, highlighting the versatile nature of this approach.

Bicontinuous interfacially jammed emulsion gels, or bijels, are a recent class of nonequilibrium soft materials formed by arrested spinodal phase separation of partially miscible fluids; colloidal particles with neutral wetting properties sequester to the interface upon phase separation and get jammed when the interfacial area only just accommodates all the particles.[18,19] Hence the bijel consists of two continuous, incompatible fluid phases stabilized by a percolating particle monolayer, and these qualities make bijels excellent candidates for templating novel macroporous and composite materials.[20] Selective polymerization of one continuous fluid phase results in a cross-linked polymer scaffold whose average domain size, L, is prescribed by the colloid volume fraction in the initial suspension, ϕ. The correspondence between L and ϕ stems from the principle that higher particle loading leads to an earlier onset of interfacial jamming and smaller fluid domains in the terminal microstructure. In the present work, nanocasting in aqueous silver nitrate solution is implemented first to seed a silver nanoparticle network within the loosely cross-linked polymer phase of the bicontinuous macroporous scaffold. Upon subsequent pyrolysis of the polymer template and concurrent sintering of the silver network, a hierarchically porous silver monolith is formed (Figure 1).

We prepared bijels in cylindrical microscopy vials of 5 mm i.d. through arrested spinodal decomposition of water and 2,6-lutidine by fluorescent Stöber silica colloids. Selective polymerization of the

Received: February 22, 2011
Published: March 31, 2011

ACS Publications © 2011 American Chemical Society

dx.doi.org/10.1021/ja201650z | J. Am. Chem. Soc. 2011, 133, 6945–6947

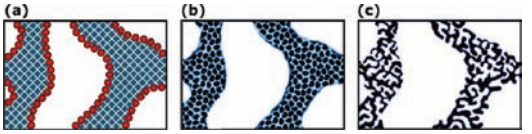

Figure 1. A nanocasting approach to hierarchically porous metals. A macroporous polymer monolith with a nanoporous polymer phase is formed from a colloidal bijel (a). The particles are etched from the surface, and silver is deposited into the polymer phase by reduction of silver ions in aqueous media (b). The polymer template is removed by pyrolysis while sintering the silver nanoparticles, resulting in a hierarchically porous monolith (c).

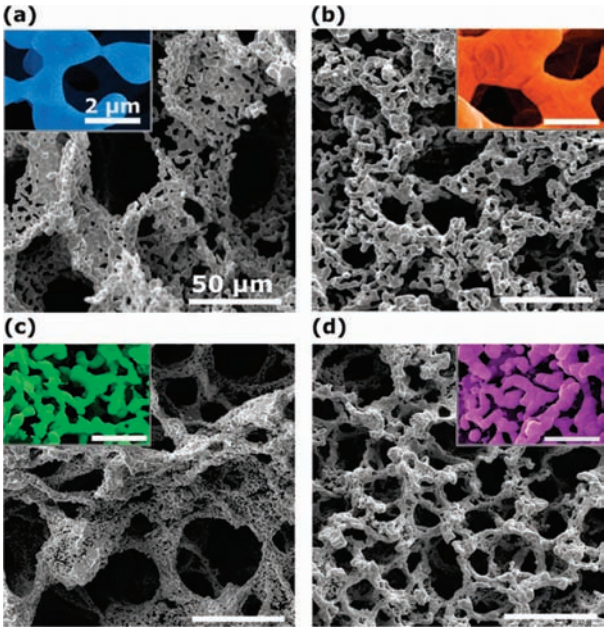

Figure 2. SEM images of hierarchical pore configurations in nanocasted silver monoliths. The inset images show the solid phase of the macroporous material in high magnification. The size of macropores/micropores may be controlled independently; shown here are examples of large/large (a), small/large (b), large/small (c), and small/small (d) pore sizes.

lutidine-rich phase was carried out by placing a small (~40 μL) layer of poly(ethylene glycol) diacrylate (PEGDA, M_w ~258) mixed with a photoinitiator (Darocur 1173) on the top surface of the ~1 cm tall bijel for 4 h while keeping the mixture sealed at 60 °C. We chose PEGDA with a low molecular weight to meet two important criteria: first, to allow its selective partitioning and dissolution into one (in this case, the organic) fluid phase; second, to ensure that the cross-linked polymer would be sufficiently wettable by aqueous solvents (see below). Molecular exchange between the oligomer layer and the lutidine-rich phase resulted in a modified bijel consisting of a dilute PEGDA-in-organic and a water-rich phase, separated by a monolayer of jammed silica particles. Photoinitiated cross-linking of the oligomer followed by solvent draining and evaporation produced a macroporous polymer monolith. Here, the cross-linked polymer phase is itself porous on a much smaller length scale, owing to the low concentration of oligomer in the fluid channels prior to cross-linking. The silica particles were etched from the internal surfaces with hydrofluoric acid, followed by thorough rinsing with water. Samples were briefly treated with aqueous sodium hydroxide and rinsed with ethanol, and the wet scaffolds were infiltrated with a

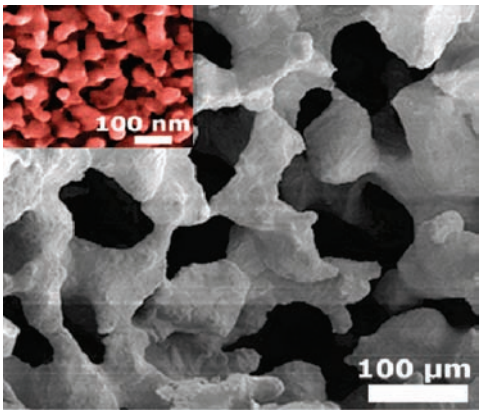

Figure 3. SEM images of a silver monolith with continuous pores on two widely separated length scales.

solution of aqueous silver nitrate and formaldehyde as a reducing agent. The white polymer monoliths turned black immediately upon contact with the silver solution, indicating the reduction of silver ions. The rate of this process was greatly enhanced by the base treatment step, which provided robust reducing conditions at the interior of the polymer phase.[21] As mentioned earlier, the choice of PEGDA scaffolds led to good wetting properties for the silver solution and allowed for uniform deposition of silver nanoparticles within the samples, which were several millimeters thick.

For clarity, we will refer to the large and small pore networks as macropores and micropores, respectively. The macropore size (L) was adjusted by the colloid volume fraction (ϕ) used in bijel formation as described earlier. Independently, the characteristic size of the micropores (l) was tuned by adjusting the cross-linked polymer density, the amount of silver nanoparticles deposited into the polymer mesh, and the sintering protocol used to remove the polymer template. Generally, longer exposure to the silver nitrate solution and lower sintering temperatures resulted in thicker solid domains with smaller micropores. These modes of morphology control enabled us to independently tune L and l, as well as the pore size ratio, η, defined as $\eta = L/l$, and here we demonstrate several possible macropore/micropore permutations in Figure 2.

A polymer template prepared from a suspension with $\phi = 3\%$ was treated with the silver precursor for 1.5 h and sintered at 520 °C, resulting in a porous silver monolith with large values of both L and l; the macropores were tens of micrometers across, and the micropores were narrower by about an order of magnitude ($\eta \approx 15$, Figure 2a). When the same procedure was carried out using a template made from a suspension with $\phi = 5\%$, the resultant macropores and micropores were much closer in size ($\eta \approx 5$) with no consequence to the underlying 3D bicontinuous morphology (Figure 2b, Supporting Information). Increasing the duration of nanocasting to 3 h and sintering the material at 370 °C reduced l to the submicrometer scale and increased η for both template sizes ($\eta \approx 100$ and 50, Figure 2c, 2d). To demonstrate the breadth of available pore sizes and the maximum value of η presently attainable with our method, a template with $L \approx 100$ μm ($\phi = 0.5\%$) was treated for 8 h and sintered at 370 °C; the large macropores were retained while generating micropores just tens of nanometers in size ($\eta \approx 2000$, Figure 3). We observed that sintering at higher temperatures tended to close the smaller pores and generate smooth walls throughout the macroporous structure (Supporting Information). EDS analysis

dx.doi.org/10.1021/ja201650z | J. Am. Chem. Soc. 2011, 133, 6945–6947

confirmed the material composition as metallic silver for all samples (Supporting Information).

In summary, we have shown that bicontinuous silver monoliths with uniform, hierarchical pore morphology across a wide range of length scales may be synthesized from colloidal bijels and a common nanocasting procedure. The characteristic sizes of the macro- and micropore networks can be tuned independently, each over a relatively broad range, providing access to pore size ratios that span nearly 3 orders of magnitude. Though we have focused here on silver monoliths, we expect that this method will provide a facile route to a variety of technologically relevant materials (e.g., gold, nickel oxide, hydroxyapatite) with hierarchical bicontinuous architecture and will be of use in various emerging applications such as energy systems, sensors, and tissue engineering.

■ ASSOCIATED CONTENT

Supporting Information. Additional images of PEGDA templates and silver monoliths, EDS spectra, Thermogravimetric analysis (TGA), experimental procedures. This material is available free of charge via the Internet at http://pubs.acs.org.

■ AUTHOR INFORMATION

Corresponding Author
mohraz@uci.edu

■ ACKNOWLEDGMENT

A.M. acknowledges UCI for startup funds. M.N.L. acknowledges the Department of Education for a GAANN fellowship.

■ REFERENCES

(1) Pestryakov, A.; Lunin, V.; Devochkin, A.; Petrov, L.; Bogdanchikova, N.; Petranovskii, V. *Appl. Catal., A* **2002**, *227*, 125–130.
(2) Schiavon, G.; Zotti, G.; Toniolo, R.; Bontempelli, G. *Anal. Chem.* **1995**, *67*, 318–323.
(3) Jain, P.; Pradeep, T. *Biotechnol. Bioeng.* **2005**, *90*, 59–63.
(4) Walsh, D.; Arcelli, L.; Ikoma, T.; Tanaka, J.; Mann, S. *Nat. Mater.* **2003**, *2*, 386–390.
(5) Jin, R.; Yuan, J. *J. Mater. Chem.* **2005**, *15*, 4513–4517.
(6) Sisk, C.; Gill, S.; Hope-Weeks, L. *Chem. Lett.* **2006**, *35*, 814–815.
(7) Khan, F.; Eswaramoorthy, M.; Rao, C. *Solid State Sci.* **2007**, *9*, 27–31.
(8) Erlebacher, J.; Aziz, M.; Karma, A.; Dimitrov, N.; Sieradzki, K. *Nature* **2001**, *410*, 450–453.
(9) Ding, Y.; Kim, Y.; Erlebacher, J. *Adv. Mater.* **2004**, *16*, 1897–1900.
(10) Ding, Y.; Erlebacher, J. *J. Am. Chem. Soc.* **2003**, *125*, 7772–7773.
(11) Hu, Y.; Adelhelm, P.; Smarsly, B.; Hore, S.; Antonietti, M.; Maier, J. *Adv. Funct. Mater.* **2007**, *17*, 1873–1878.
(12) Su, F.; Zhao, X.; Wang, Y.; Zeng, J.; Zhou, Z.; Lee, J. *J. Phys. Chem. B* **2005**, *109*, 20200–20206.
(13) Chai, G.; Yoon, S.; Yu, J.; Choi, J.; Sung, Y. *J. Phys. Chem. B* **2004**, *108*, 7074–7079.
(14) Yuan, Z.; Su, B. *J. Mater. Chem.* **2006**, *16*, 663–677.
(15) Stein, A.; Li, F.; Denny, N. *Chem. Mater.* **2007**, *20*, 649–666.
(16) Studart, A.; Studer, J; Xu, L; Yoon, K; Shum, H. C.; Weitz, D. *Langmuir* **2010**, *27*, 955–964.
(17) Chen, H.; Kwon, Y.; Thornton, K. *Scripta. Mater.* **2009**, *61*, 52–55.
(18) Herzig, E. M.; White, K. A.; Schofield, A. B.; Poon, W. C. K.; Clegg, P. S. *Nat. Mater.* **2007**, *6*, 966–971.
(19) Stratford, K.; Adhikari, R.; Pagonabarraga, I.; Desplat, J. C.; Cates, M. E. *Science* **2005**, *309*, 2198–2201.
(20) Lee, M.; Mohraz, A. *Adv. Mater.* **2010**, *22*, 4836–4841.
(21) Chou, K.; Ren, C. *Mater. Chem. Phys.* **2000**, *64*, 241–246.